

# The Structure of $[\text{ReH}_2(\text{H}_2)(\text{CO})(\text{PMe}_3)_3]^+$ Revisited

Dmitry G. Gusev†

Department of Chemistry, Wilfrid Laurier University, Waterloo, Ontario N2L 3C5 Canada

Received July 4, 2003

**Summary:** The structure of the dihydrogen complexes  $[\text{ReH}_2(\text{H}_2)(\text{CO})\text{L}_3]^+$  ( $\text{L} = \text{PPhMe}_2, \text{PMe}_3, \text{PH}_3$ ) has been a matter of some controversy. DFT calculations carried out for  $[\text{ReH}_2(\text{H}_2)(\text{CO})(\text{PMe}_3)_3]^+$  in this work established that the most stable structure has the dihydrogen and carbonyl ligands in the axial sites of the pentagonal-bipyramidal geometry.

Experimental elucidation of the structure of polyhydrides has always been challenging. Accurate location of metal-bonded hydrogen atoms by XRD is problematic, and some polyhydride complexes are thermally unstable and difficult to crystallize. In solution, NMR spectroscopy is often unable to establish the molecular symmetry or connectivities because hydride chemical shifts and couplings can be averaged by rapid ligand exchange. A particularly controversial polyhydride system,  $[\text{ReH}_4(\text{CO})\text{L}_3]^+\text{A}^-$  ( $\text{L} = \text{PPhMe}_2, \text{A}^- = \text{BF}_4^-, \text{L} = \text{PMe}_3, \text{A}^- = \text{CF}_3\text{CO}_2^-$ ), was prepared in the beginning of the 1990s by low-temperature protonation of  $\text{ReH}_3(\text{CO})\text{L}_3$  in  $\text{CD}_2\text{-Cl}_2$ .<sup>1,2</sup> In solution, the  $[\text{ReH}_4(\text{CO})\text{L}_3]^+$  complexes form equilibrium mixtures of tetrahydrido (**1**) and dihydrido-dihydrogen (**2**) isomers, which could not be crystallized and characterized by XRD. On the basis of the VT NMR data, the structure of **1** has been agreed to be dodecahedral, as shown in Chart 1. Unfortunately, NMR spectroscopy could not unambiguously establish the structure of **2** and only indicated that the nonclassical isomer should have  $C_s$  symmetry with two phosphorus ligands and two hydrides in one plane. The reasonable molecular geometries **2a** and **2b** were assigned by the experimental chemists.<sup>1,2</sup> Subsequent computational work<sup>3</sup> (with  $\text{L} = \text{PH}_3$ ) rejected **2a** as a high-energy nonstationary point on the energy surface and (without considering **2b**) suggested that isomer **2** could have the structure **2c**.

Recent theoretical advances coupled with the rapid development of computer technology have transformed computational chemistry into a reliable technique for structural determination of transition-metal complexes.<sup>4</sup> Full incorporation of the electronic and steric effects of trialkylphosphines is now possible, which is essential to correct modeling of the experimental reality.<sup>5</sup> This prompted us to reinvestigate all isomers shown in Chart

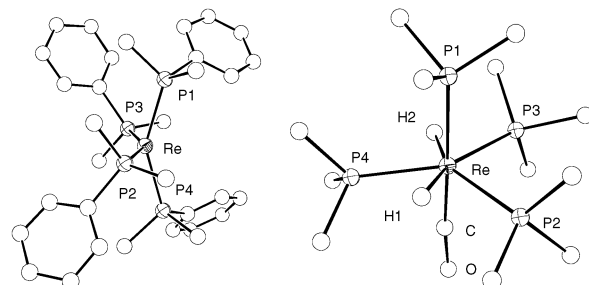
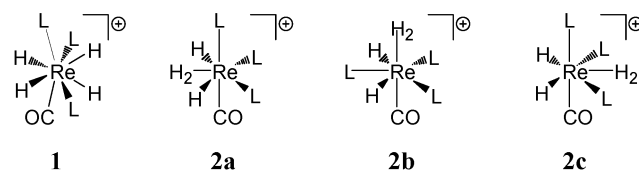


**Figure 1.** Crystal structures of  $[\text{ReH}_4(\text{PPhMe}_2)_4]^+$  and  $[\text{ReH}_2(\text{CO})(\text{PMe}_3)_4]^+$  reconstructed from the coordinates reported in refs 6 and 2a. All nonmetal hydrogen atoms are omitted for clarity. Hydrides were not located in the tetrahydride.

## Chart 1



1 for  $[\text{ReH}_2(\text{H}_2)(\text{CO})(\text{PMe}_3)_3]^+$  by employing DFT calculations with good-quality basis sets and without constraints.

To generate realistic models of complexes **1** and **2** for geometry optimizations, we first considered the crystal structures of two related rhenium compounds:  $[\text{ReH}_4(\text{PPhMe}_2)_4]^+$  and  $[\text{ReH}_2(\text{CO})(\text{PMe}_3)_4]^+$ , shown in Figure 1.<sup>2a,6</sup> In the tetrahydride, replacing all phenyls by methyl groups and substituting a carbonyl for one phosphine afforded the starting geometry for **1** (with the four hydrides placed in the idealized positions to complete the dodecahedron). Starting geometries for **2a** and **2b** were derived from  $[\text{ReH}_2(\text{CO})(\text{PMe}_3)_4]^+$  by substituting  $\text{H}_2$  for  $\text{PMe}_3$ , labeled in Figure 1 as P4 and P1, respectively. An appropriate model for **2c** was obtained from **1** by shortening the distance between the two H atoms in the P–Re–CO plane.

A series of preliminary calculations were carried out for the dihydride  $[\text{ReH}_2(\text{CO})(\text{PMe}_3)_4]^+$  to evaluate the performance of three DFT methods, as well as the effect of the chosen basis sets bs1 and bs2 (see the Experimental Section for details). The X-ray crystallographic and computational results for  $[\text{ReH}_2(\text{CO})(\text{PMe}_3)_4]^+$  are presented in Table 1 and show a good agreement for all bond angles, regardless of the computational method used. The Re–P distances were best predicted at the  $m\text{PW1PW91}$  level, which overestimated the distances

(6) Lunder, D. M.; Green, M. A.; Streib, W. E.; Caulton, K. G. *Inorg. Chem.* **1989**, *28*, 4527.

† E-mail: dgoussev@wlu.ca.

(1) Luo, X.-L.; Crabtree, R. H. *Chem. Commun.* **1990**, 189. (b) Luo, X.-L.; Crabtree, R. H. *J. Am. Chem. Soc.* **1990**, *112*, 6912.

(2) (a) Gusev, D. G.; Nietlispach, D.; Eremenko, I. L.; Berke, H. *Inorg. Chem.* **1993**, *32*, 3628. (b) Gusev, D. G.; Berke, H. *Chem. Ber.* **1996**, *129*, 1143.

(3) Lin, Z.; Hall, M. B. *J. Am. Chem. Soc.* **1994**, *116*, 4446.

(4) (a) Ziegler, T. *J. Chem. Soc., Dalton Trans.* **2002**, 642. (b) Maseras, F.; Lledós, A.; Clot, E.; Eisenstein, O. *Chem. Rev.* **2000**, *100*, 601.

(5) (a) Clot, E.; Eisenstein, O. *J. Phys. Chem. A* **1998**, *102*, 3592. (b) Jacobsen, H.; Berke, H. *Chemistry* **1997**, *3*, 881.

**Table 1.** Selected Experimental and Calculated Bond Distances and Angles<sup>a</sup> for [ReH<sub>2</sub>(CO)(PMe<sub>3</sub>)<sub>4</sub>]<sup>+</sup>

method	Re–P <sub>av</sub>	Re–C	C–O	P1–Re–P4	P2–Re–P3	P3–Re–P4	P1–Re–P2	P1–Re–C	P3–Re–C	P4–Re–C
B3LYP/bs2 <sup>b</sup>	2.510	1.93	1.17	98.1	91.9	134.5	92.1	179.3	88.5	81.3
B3PW91/bs2	2.477	1.92	1.17	98.2	92.5	133.8	92.3	179.2	88.6	81.1
<i>m</i> PW1PW91/bs2	2.466	1.92	1.17	98.2	92.2	134.1	92.1	179.2	88.7	81.1
<i>m</i> PW1PW91/bs1 <sup>c</sup>	2.470	1.90	1.17	98.6	93.0	133.8	92.1	179.4	88.5	80.9
X-ray	2.425(6)	1.81(3)	1.24(3)	99.4(2)	91.6(2)	132.7(2)	91.3(2)	177.6(8)	91.1(8)	78.8(7)

<sup>a</sup> Bond distances are given in angstroms and bond angles in degrees. <sup>b</sup> Basis set bs2: SDD + ECP (Re), 6-31G(p) (hydrides), 6-31G(d) (all other atoms). <sup>c</sup> Basis set bs1: LANL2DZ (with ECP's for Re and P, augmented with single polarization functions on CO and all atoms bonded to Re).

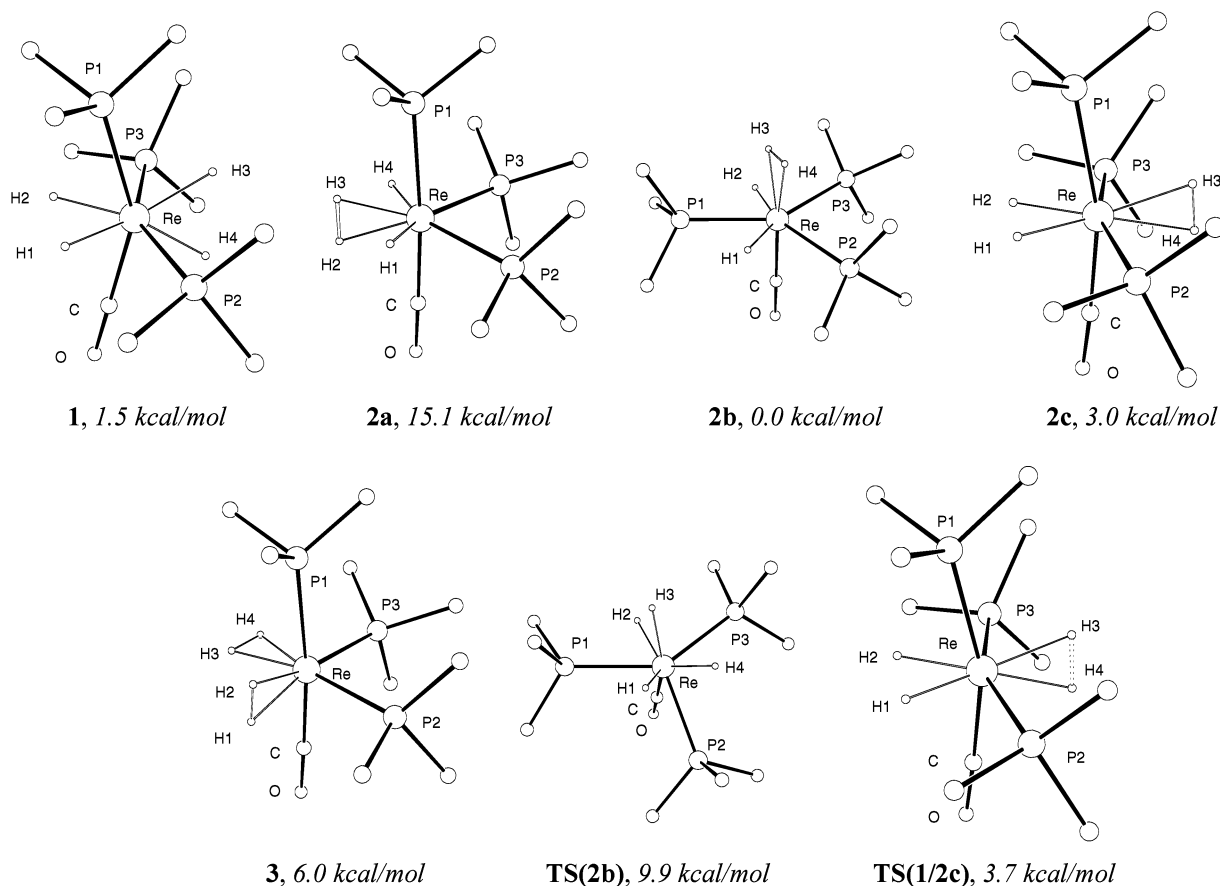


**Figure 2.** Theoretical structures of [ReH<sub>4</sub>(CO)(PMe<sub>3</sub>)<sub>3</sub>]<sup>+</sup> optimized at the *m*PW1PW91/bs1 level for **TS(2b)** and **TS(1/2c)** and at the *m*PW1PW91/bs2 level for isomers **1–3**. All nonmetal hydrogen atoms are omitted for clarity. All energies are relative to that of **2b** and were calculated at the *m*PW1PW91/bs3 level.

by 0.041 Å on average, exceeding the experimental crystallographic error ( $3\sigma = 0.018$  Å). The calculated Re–C and C–O distances are also longer than the crystallographic values, although the differences of 0.09 and 0.07 Å are within  $3\sigma = 0.09$  Å and statistically may not be meaningful. It should be noted that the distances calculated for [ReH<sub>2</sub>(CO)(PMe<sub>3</sub>)<sub>4</sub>]<sup>+</sup> are close to those in the dihydride of a very similar overall structure, ReH<sub>2</sub>(CO)(SiPh<sub>3</sub>)(PPhMe<sub>2</sub>)<sub>3</sub>, where Re–C = 1.88(1) Å and C–O = 1.16(1) Å.<sup>7</sup> Table 1 shows a negligible effect of the basis sets bs1 and bs2. It has been suggested that the *m*PW1PW91 functional is superior in describing weak interactions (which is important in the case of H<sub>2</sub> coordination); it also better represents the energies compared to the widely used B3LYP functional.<sup>8</sup> Therefore, in this work, the *m*PW1PW91/bs1 approach was

used for all geometry optimizations and frequency calculations on [ReH<sub>4</sub>(CO)(PMe<sub>3</sub>)<sub>3</sub>]<sup>+</sup>. Isomers **1–3** were additionally optimized at the *m*PW1PW91/bs2 level without frequency calculations, and their electronic energies were calculated at the *m*PW1PW91/bs3 level, as described in the Experimental Section.

Main computational results of this work, presented in Figure 2 and Table 2, show that the dihydrogen complex **2b** and tetrahydride **1** are the two most stable species among the isomers of [ReH<sub>4</sub>(CO)(PMe<sub>3</sub>)<sub>3</sub>]<sup>+</sup>. Theoretically, **1** lies 1.5 kcal/mol higher than **2b**; however, in solution, **1** is known to be ca. 1 kcal/mol more stable than the nonclassical isomer.<sup>2</sup> In addressing this minor inconsistency, it should be remembered that energy differences within 3 kcal/mol in DFT calculations should certainly be treated very cautiously,<sup>4,5,9</sup> particu-

(7) Luo, X.-L.; Schulte, G. K.; Demou, P.; Crabtree, R. H. *Inorg. Chem.* **1990**, *29*, 4268.

(8) (a) Poremski, M.; Weisshaar, J. C. *J. Phys. Chem. A* **2001**, *105*, 4851. (b) Lynch, B. J.; Truhlar, D. G. *J. Phys. Chem. A* **2001**, *105*, 2936. (c) Trage, C.; Schröder, D.; Schwarz, H. *Organometallics* **2003**, *22*, 693.

(9) (a) Koch, W.; Holthausen, M. C. *A Chemist's Guide to Density Functional Theory*; Wiley-VCH: Weinheim, Germany, 2000. (b) Diedenhofen, M.; Wagener, T. M.; Frenking, G. In *Computational Organometallic Chemistry*; Cundari, T. R., Ed.; Marcel Dekker: Basel, Switzerland, 2001.

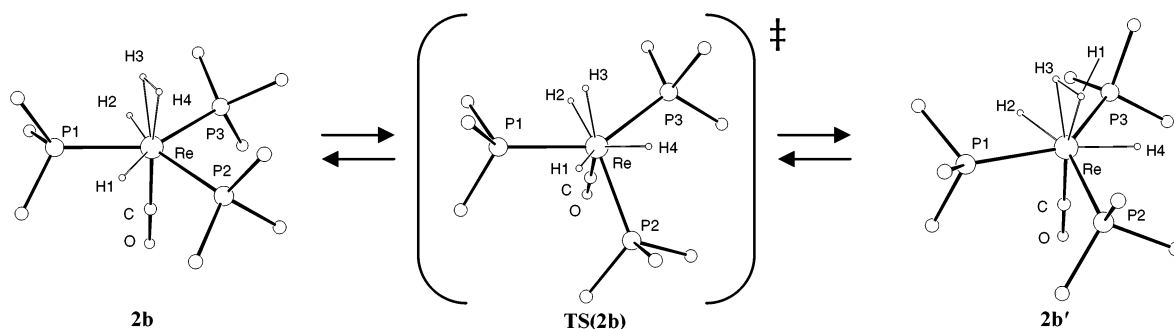


**Figure 3.** Schematic depiction of the dynamic process operating in **2b** and resulting in the simultaneous chemical shift exchange in the  $^{31}\text{P}$  and  $^1\text{H}$  NMR spectra of  $[\text{ReH}_2(\text{H}_2)(\text{CO})(\text{PMe}_3)_3]^+$ .

**Table 2.** Selected Bond Distances and Angles<sup>a</sup> for the Theoretical Structures in Figure 2

distance/ angle	<b>1</b>	<b>2a</b>	<b>2b</b>	<b>2c</b>	<b>3</b>	TS( <b>2b</b> )	TS( <b>1/2c</b> )
H–H		0.94	0.85	0.91	0.88		1.09
H1⋯H2	1.82	2.00		1.49	0.91	<i>b</i>	1.63
Re–H1	1.68	1.68	1.69	1.66	1.79	1.67	1.66
Re–H2	1.68	1.72	1.69	1.66	1.79	1.68	1.66
Re–H3	1.69	1.73	1.83	1.79	1.76	1.66	1.73
Re–H4	1.68	1.68	1.84	1.79	1.76	1.67	1.72
Re–P1	2.467	2.484	2.407	2.470	2.491	2.427	2.478
Re–P2	2.456	2.486	2.478	2.466	2.434	2.487	2.466
Re–P3	2.455	2.488	2.479	2.465	2.438	2.428	2.464
Re–C	1.975	1.947	1.922	1.949	1.945	1.982	1.933
P1–Re–P2	95.5	97.5	132.3	94.4	96.7	107.8	94.8
P1–Re–P3	96.0	93.7	137.3	94.3	93.6	142.2	95.0
P2–Re–P3	149.4	90.5	90.5	160.6	94.4	109.1	156.6
P1–Re–C	151.3	175.3	89.1	166.0	173.2	90.4	162.1

<sup>a</sup> Bond distances are given in angstroms and angles in degrees.

<sup>b</sup> H⋯H distances (Å) in **TS(2b)**: H1⋯H3 = 1.96, H1⋯H4 = 1.84, H3⋯H2 = 1.86, H3⋯H4 = 1.99 Å.

larly when solvent, ion-pairing effects, or entropy effects are not taken into consideration.

Dihydrogen complex **2b** in Figure 2 has a short H3–H4 bond of 0.85 Å, in agreement with the 0.86 Å value calculated<sup>10</sup> from the experimental  $^1J_{\text{HD}}$  constant of 33.6 Hz.<sup>2a</sup> The H<sub>2</sub> ligand of **2b** is trans to the carbonyl and is significantly removed from the metal center (Re–H3 = 1.83 Å vs Re–H1 = 1.69 Å), which is consistent with the thermal instability of **2** and its facile decomposition by H<sub>2</sub> loss. The structure **2b** has the three most bulky ligands in the pentagonal plane of the bipyramidal geometry. This feature makes its low energy counterintuitive and may explain why such an isomer was not considered by the experimental chemists for  $[\text{ReH}_2(\text{H}_2)(\text{CO})(\text{PPhMe}_2)_3]^+$  and by the theoreticians for  $[\text{ReH}_2(\text{H}_2)(\text{CO})(\text{PH}_3)_3]^+$ . Unfortunately, the process of establishing a nontrivial structure by NMR spectroscopic and theoretical means is often guided by intuition and as such may not be all-inclusive.

Geometry optimizations toward **2a** resulted in two different structures. The mono(dihydrogen) product (**2a** in Figure 2) was obtained when the initial model had the H2–H3 bond eclipsing the P1–C axis. When the calculation was started with the H2–H3 ligand in the H1–Re–H4 plane, it converged to the d<sup>6</sup> octahedral bis(dihydrogen) complex  $[\text{Re}(\text{H}_2)_2(\text{CO})(\text{PMe}_3)_3]^+$  (**3**). Obvi-

ously, **2a** is the least likely isomer of  $[\text{ReH}_2(\text{H}_2)(\text{CO})(\text{PMe}_3)_3]^+$ , since it lies 13.6 kcal/mol higher than **1**. This is in agreement with the previous MP2 calculations,<sup>3</sup> where the corresponding structure of  $[\text{ReH}_2(\text{H}_2)(\text{CO})(\text{PH}_3)_3]^+$  was located 12.1 kcal/mol above the tetrahydride isomer. It can be noted that if complex **2a** had formed as a kinetic product of the protonation of  $\text{ReH}_3(\text{CO})(\text{PMe}_3)_3$ , it should have spontaneously isomerized into the lower energy bis(dihydrogen) structure **3** upon rotation of the H<sub>2</sub> ligand.

Finally, the structure **2c** was calculated and found to be 1.5 kcal/mol less stable than **1**, which is consistent with the small 0.2 kcal/mol gap between the corresponding isomers of  $[\text{ReH}_4(\text{CO})(\text{PH}_3)_3]^+$  and  $[\text{ReH}_2(\text{H}_2)(\text{CO})(\text{PH}_3)_3]^+$ , optimized at the MP2 level.<sup>3</sup> Figure 2 also shows a transition structure connecting **1** and **2c**, **TS(1/2c)**, which lies 2.2 kcal/mol above **1**. From the previous MP2 calculations, the energy of **TS(1/2c)** (with L = PH<sub>3</sub>) was estimated as 4 kcal/mol.<sup>3</sup> Given the very low energy barrier, structures **1** and **2c** should exist in a rapid equilibrium on the NMR time scale in solution. The experimental observation of three resonances in the hydride region of the low-temperature  $^1\text{H}$  NMR spectra of **1** and **2** is, therefore, incompatible with the structural interpretation of  $[\text{ReH}_2(\text{H}_2)(\text{CO})(\text{PMe}_3)_3]^+$  as **2c**.

Thus far, the computational results have strongly suggested that structure **2b** most likely corresponds to that of  $[\text{ReH}_2(\text{H}_2)(\text{CO})(\text{PMe}_3)_3]^+$  in solution.<sup>11</sup> We thought we should also try to explain how this dihydrogen complex could be highly fluxional in both  $^1\text{H}$  and  $^{31}\text{P}$  NMR spectra, where the exchange occurred at the same rate, apparently implying a common mechanism. A transition structure for this exchange (**TS(2b)** in Figure 3) was calculated and found to lie 9.9 kcal/mol higher than **2b**, in an excellent agreement with the experimental value for the exchange barrier,  $\Delta G^\ddagger = 8.6\text{--}8.7$  kcal/mol.<sup>2</sup> The optimized **TS(2b)** has an overall C<sub>s</sub>-symmetric geometry derived from **2b** by cleaving the H3–H4 bond and making H1 and H4 equidistant from the H2–H3–P2 plane. When **TS(2b)** was distorted toward the product and optimized in search of a minimum, the calculation converged to **2b'**. Inspection of **2b** and **2b'** in Figure 3 shows that the two molecules are isostructural and are related by ligand exchange. Particularly, H1 is a hydride and H4 is in the coordinated dihydrogen

(11) Following a reviewer's suggestion, we also optimized an isomer of  $[\text{ReH}_2(\text{H}_2)(\text{CO})(\text{PMe}_3)_3]^+$  (**2d**) containing the H<sub>2</sub> ligand trans to PMe<sub>3</sub> in the axial sites of the bipyramidal geometry. The energy of **2d**, calculated at the *m*PW1PW91/bs2 level, is 12.9 kcal/mol relative to that of **2b**. Full computational details and a figure showing the structure of **2d** have been included in the Supporting Information.

(10) Maltby, P. A.; Schlaf, M.; Steinbeck, M.; Lough, A. J.; Morris, R. H.; Klooster, W. T.; Koetzle, T. F.; Srivastava, R. C. *J. Am. Chem. Soc.* **1996**, *118*, 5396.

in **2b**, whereas in **2b'** it is the other way around: H1 is in the dihydrogen and H4 is a hydride, and their  $^1\text{H}$  chemical shifts are swapped. Simultaneously, the two phosphine ligands P1 and P3 exchange their environments and, hence, the chemical shifts. In a similar way, the exchange process shown in Figure 3 will also involve H2/H3 and P1/P2 when the dihydrogen ligand is reoriented (by rotation) to lie along the Re–P3 bond.

### Conclusions

Complex **2b** is theoretically the most stable of the isomers of  $[\text{ReH}_2(\text{H}_2)(\text{CO})(\text{PMe}_3)_3]^+$ , and its calculated structure is believed to closely represent the molecular geometry of this complex in solution. Facile intramolecular exchange of the metal-bonded hydrogen and phosphorus atoms in  $[\text{ReH}_2(\text{H}_2)(\text{CO})(\text{PMe}_3)_3]^+$  can proceed via the  $C_s$ -symmetric transition state **TS(2b)**.

### Experimental Section

The calculations were carried out on a dual 2.4 GHz Xeon workstation with Gaussian 98 (revision A.11) and GaussView (version 2) programs.<sup>12</sup> All geometries were fully optimized without symmetry or internal coordinate constraints using the *mPW1PW91* functional, which included modified Perdew–

Wang exchange and Perdew–Wang 91 correlation.<sup>13</sup> Two basis sets were employed for the geometry optimizations: bs1 included LANL2DZ augmented by single polarization functions for CO and all metal-bonded atoms and associated with the ECP's for Re and P; bs2 included SDD (associated with an ECP) for Re, 6-31G(p) for the hydrides, and 6-31G(d) for all other atoms.<sup>14</sup> All geometries were optimized at the *mPW1PW91/bs1* level, and the nature of the stationary points was verified by frequency calculations, which were also used to calculate ZPE without scaling. Synchronous transit-guided quasi-Newton (STQN) methods<sup>15</sup> QST3 and QST2 were used to optimize transition states **TS(2b)** and **TS(1/2c)**, respectively. Motions corresponding to the single imaginary frequencies were visually checked. Complexes **1–3** were also optimized at the *mPW1PW91/bs2* level, using the atomic coordinates and force constants provided by the *mPW1PW91/bs1* calculations. All reported energies are ZPE-corrected and originate from single-point *mPW1PW91/bs3* calculations using the SDD + ECP basis set for Re and the 6-31+G(d, p) basis set for all other atoms.

**Acknowledgment.** Financial support from the NSERC and Research Corp. is gratefully acknowledged.

**Supporting Information Available:** Tables giving atomic coordinates and energies of the optimized complexes **1–3**. This material is available free of charge via the Internet at <http://pubs.acs.org>.

OM034017C

(12) Frisch, M. J.; Trucks, G. W.; Schlegel, H. B.; Scuseria, G. E.; Robb, M. A.; Cheeseman, J. R.; Zakrzewski, V. G.; Montgomery, J. A., Jr.; Stratmann, R. E.; Burant, J. C.; Dapprich, S.; Millam, J. M.; Daniels, A. D.; Kudin, K. N.; Strain, M. C.; Farkas, O.; Tomasi, J.; Barone, V.; Cossi, M.; Cammi, R.; Mennucci, B.; Pomelli, C.; Adamo, C.; Clifford, S.; Ochterski, J.; Petersson, G. A.; Ayala, P. Y.; Cui, Q.; Morokuma, K.; Malick, D. K.; Rabuck, A. D.; Raghavachari, K.; Foresman, J. B.; Cioslowski, J.; Ortiz, J. V.; Stefanov, B. B.; Liu, G.; Liashenko, A.; Piskorz, P.; Komaromi, I.; Gomperts, R.; Martin, R. L.; Fox, D. J.; Keith, T.; Al-Laham, M. A.; Peng, C. Y.; Nanayakkara, A.; Gonzalez, C.; Challacombe, M.; Gill, P. M. W.; Johnson, B. G.; Chen, W.; Wong, M. W.; Andres, J. L.; Head-Gordon, M.; Replogle, E. S.; Pople, J. A. *Gaussian 98*, revision A.11; Gaussian, Inc.: Pittsburgh, PA, 1998.

(13) (a) Adamo, C.; Barone V. *J. Chem. Phys.* **1998**, *108*, 664. (b) Perdew, J. P.; Burke, K.; Wang, Y. *Phys. Rev. B* **1996**, *54*, 16533. (c) Burke, K.; Perdew, J. P.; Wang, Y. In *Electronic Density Functional Theory: Recent Progress and New Directions*; Dobson, J. F., Vignale, G., Das, M. P., Eds.; Plenum: New York, 1998.

(14) The basis sets are available from the Extensible Computational Chemistry Environment Basis Set Database, which has been developed and distributed by the Molecular Science Computing Facility, Environmental and Molecular Sciences Laboratory, a part of the Pacific Northwest Laboratory, P.O. Box 999, Richland, WA 99352.

(15) Peng, C.; Ayala, P. Y.; Schlegel, H. B.; Frisch, M. J. *J. Comput. Chem.* **1996**, *17*, 49.